Latin American Journal of Solids and Structures
www.lajss.org

A Comuputerized DRBEM model for generalized magneto-thermo-visco-elastic stress waves in functionally graded anisotropic thin film/substrate structures

Abstract

A numerical computer model, based on the dual reciprocity boundary element method (DRBEM) for studying the generalized magneto-thermo-visco-elastic stress waves in a rotating functionally graded anisotropic thin film/substrate structure under pulsed laser irradiation is established. An implicit-implicit staggered algorithm was proposed and implemented for use with the DRBEM to get the solution for the temperature, displacement components and thermal stress components through the structure thickness. A comparison of the results for different theories is presented in the presence and absence of rotation. Some numerical results that demonstrate the validity of the proposed method are also presented.

Keywords

Magneto-Thermoviscoelasticity; Rotation; Functionally graded materials; Anisotropic; Dual Reciprocity Boundary Element Method; Distribution.

Mohamed Abdelsabour Fahmy[a,b,*]

[a]Mathematics Department, University College, Umm Al-Qura University, Makkah, The Kingdom of Saudi Arabia
[b]Basic Sciences Department, Faculty of Computers and Informatics, Suez Canal University, Ismailia, Egypt

Received in 22 Feb 2013
In revised form 10 Jul 2013

[*]Author email:
mohamed_fahmy@ci.suez.edu.eg

1 INTRODUCTION

Biot (1956) introduced the theory of coupled thermoelasticity to overcome the first shortcoming in the theory of uncoupled thermoelasticity introduced by Duhamel (1837) and Neuman (1885) where it predicts two phenomena not compatible with physical observations. First, the equation of heat conduction of this theory does not contain any elastic terms. Second, the heat equation is of a parabolic type, predicting infinite speeds of propagation for heat waves. Later on, generalized theories of thermoelasticity were introduced in order to eliminate the shortcomings of the uncoupled thermoelasticity. Lord and Shulman (1967) developed the theory of coupled thermoelasticity with one relaxation time by constructing a new law of heat conduction to replace the classical Fourier's law. This law contains the heat flux vector as well as its time derivative. It contains also new constant that acts as relaxation time. Since the heat equation of this theory is of the wave-type, it automatically ensures finite speeds of propagation for heat and elastic waves. Green and Lindsay (1972) in-

cluded a temperature rate among the constitutive variables to develop a temperature–rate-dependent thermoelasticity that does not violate the classical Fourier's law of heat conduction when the body under consideration has a center of symmetry; this theory also predicts a finite speed of heat propagation. This theory is known as the theory of thermoelasticity with two relaxation times. According to these theories, heat propagation should be viewed as a wave phenomenon rather than diffusion one Relevant theoretical developments on the subject were made by Green and Naghdi (1992, 1993) they developed three models for generalized thermoelasticity of homogeneous isotropic materials which are labeled as model I, II and III. These theories of thermoelasticity LS, GL and GN theories are known as the generalized theories of thermoelasticity with finite thermal wave speed. In general, it is not easy to obtain analytical solutions to a dynamical magneto-thermo-visco-elastic problem in anisotropic materials. therefore, an important number of engineering and mathematical papers devoted to the numerical solution have studied the overall behavior of such materials (Oden and Armstrong, 1971; Ting and Chen, 1982; Dargush and Banerjee, 1991; Misra, et al., 1992; Chen, et al., 2009; Tsai, 2009; Xing and Makinouchi, 2002; El-Naggar, et al., 2002, 2004; Abd-Alla, et al., 2003, 2007, 2008; Wu and Chu, 2004; Baksi, et al., 2006; Hosseini, et al., 2007; Huang and Rosakis, 2007; Fahmy, 2008, 2009; Fahmy and El-Shahat, 2008; Feng, et al., 2008; Othman and Song, 2008; Damanpack, et al. (2013); Rafieipour, et al. (2013)).

Recently, generalized thermoelastic functionally graded thin films (FGTFs) have been attracting much attention for a wide variety of potential optical and electronic applications, including memory devices, solar cells, optoelectronic devices, bio/chemical sensors, semiconductor devices, transparent conductors, surface acoustic wave devices, optical modulator devices and integrated optic devices, because of their high dielectric constants, large spontaneous polarizations,and large pyroelectric, piezoelectric and electro optic effect. So it is very important and necessary to study the magneto-thermoviscoelastic stress waves in the film/substrate structures. Interested readers can find more details and applications of thin films in the following references (Chen and Chung, 1995; Cherepanov and Martinez, 1997; Zhou et al., 2006; Hsueh et al., 2010; Chang, 2011).

To deal with an arbitrary body force in elasticity, Nardini and Brebbia (1983) developed a procedure nowadays known as the dual reciprocity boundary element method (DRBEM). The purpose of the DRBEM is to convert the domain integral into a boundary one. This method was initially developed in the context of two-dimensional (2D) elastodynamics and has been extended to deal with a variety of problems wherein the domain integral may account for linear-nonlinear static-dynamic effects. The DRBEM has been highly successful in a very wide range of engineering applications, including acoustics, aeroacoustics, aerodynamics, fluid dynamics, fracture analysis, geomechanics, elasticity and heat transfer. A more extensive historical review and applications of dual reciprocity boundary element method may be found in (Brebbia et al., 1984; Wrobel and Brebbia, 1987; Partridge and Brebbia, 1990; Partridge and Wrobel, 1990; Partridge et al., 1992; Gaul et al., 2003; Lu and Wu, 2006; Fahmy, 2010, 2011, 2011a, 2012).

The main aim of this paper is to study the propagation of magneto-thermo-visco-elastic stress waves through the thickness of the anisotropic functionally graded (FG) thin film/substrate structure when it is rotated about the y-axis under pulsed laser irradiation. An implicit-implicit staggered strategy was developed and implemented for use with the DRBEM to obtain the solution for the displacement and temperature fields. Numerical computations for the temperature, displace-

ment components and thermal stress components are carried out and represented graphically. Comparisons are made with the results predicted by the four theories (LS model, GL model, GN model II, GN model III) in the presence and absence of rotation. Some numerical results that demonstrate the validity of the proposed method are also presented.

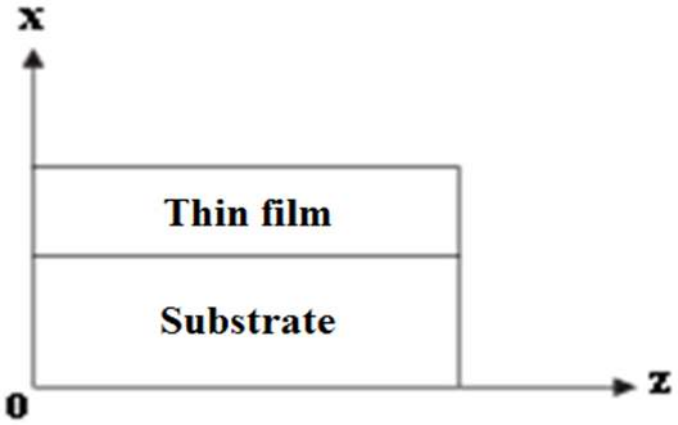

Figure 1 Geometry of the problem

2 FORMULATION OF THE PROBLEM

The structure consists of an anisotropic FG thin film of thickness h and an anisotropic FG substrate with thickness d in the Cartesian coordinate system $(\mathrm{x},\mathrm{y},\mathrm{z})$ is considered as shown in Fig. 1. This structure is placed in a primary magnetic field H_0 acting in the direction of the y-axis and rotating about it with a constant angular velocity in the presence of pulsed laser irradiation. Here we address the generalized two-dimensional deformation problem in xz-plane only, where the structure occupies the region $\mathrm{R} = \{(x,z): 0 < x < \bar{\mathrm{d}} + \bar{\mathrm{h}}, 0 < z < a\}$ which is bounded by a simple closed curve C. At each and every point on the boundary C, the temperature and displacement are suitably specified.

According to Lord-Shulman (LS), Green-Lindsay (GL) and Green-Naghdi (GN) theories, the governing equations of generalized magneto-thermo-viscoelasticity in a rotating anisotropic FG thin film/substrate structure, can be written in the following unified form:

$$\sigma_{ab,b} + \tau_{ab,b} - \bar{\rho}^{i}\omega^{2}x_{a} = \bar{\rho}^{i}\ddot{u}^{i}_{a} \tag{1}$$

$$\sigma_{ab} = \aleph\left[\bar{C}^{i}_{abfg}u^{i}_{f,g} - \bar{\beta}^{i}_{ab}(T^{i} - T_0 + \tau_1\dot{T}^{i})\right], \qquad \bar{C}^{i}_{abfg} = \bar{C}^{i}_{fgab} = \bar{C}^{i}_{bafg}, \bar{\beta}^{i}_{ab} = \bar{\beta}^{i}_{ba} \tag{2}$$

$$\tau_{ab} = \bar{\mu}^{i}\left(\tilde{h}_{a}H_{b} + \tilde{h}_{b}H_{a} - \delta_{ba}(\tilde{h}_{f}H_{f})\right), \qquad \tilde{h}_{a} = \left(\nabla\times\left(u^{i}\times H\right)\right)_{a} \tag{3}$$

$$\begin{aligned}&\left[\delta_{1j}\bar{k}^{i}_{ab} + \delta_{2j}\bar{k}^{i*}_{ab}\right]T^{i}_{,ab} + \bar{\rho}^{i}(\ddot{\mathfrak{X}} + \tau_0\dot{\mathfrak{X}})\\ &= -\delta_{2j}\bar{k}^{i}_{ab}\dot{T}^{i}_{,ab} + \bar{\beta}^{i}_{ab}T_0\left[\mathring{A}\delta_{1j}\dot{u}^{i}_{a,b} + (\tau_0 + \delta_{2j})\ddot{u}^{i}_{a,b}\right]\\ &+\bar{\rho}^{i}\bar{c}^{i}\left[\delta_{1j}\dot{T}^{i} + (\tau_0 + \delta_{1j}\tau_2 + \delta_{2j})\ddot{T}^{i}\right]\end{aligned} \tag{4}$$

where σ_{ab} is the mechanical stress tensor, τ_{ab} Maxwell's electromagnetic stress tensor, u_k^i is the displacement, T_0 is the reference temperature, T^i is the temperature, $\bar{C}_{abfg}^i$ and $\bar{\beta}_{ab}^i$ are respectively, the constant elastic moduli and stress-temperature coefficients of the anisotropic medium, $\aleph = \left(1 + \nu_0 \frac{\partial}{\partial \tau}\right)$ is the viscoelastic material constant, ν_0 is the viscoelastic relaxation time, $\bar{\mu}^i$ is the magnetic permeability, $\tilde{h}$ is the perturbed magnetic field, ω is the uniform angular velocity, $\bar{k}_{ab}^i \left(\bar{k}_{ab}^i = \bar{k}_{ba}^i, \left(\bar{k}_{12}^i\right)^2 - \bar{k}_{11}^i \bar{k}_{22}^i < 0\right)$ are the thermal conductivity coefficients, $\bar{k}_{ab}^{i*}$ ($\bar{k}_{ab}^{i*} = \bar{k}_{ba}^{i*}, \left(\bar{k}_{12}^{i*}\right)^2 - \bar{k}_{11}^{i*} \bar{k}_{22}^{i*} < 0$) is the second order tensor of new material constants associated with the GN theories, $\bar{\rho}^i$ is the density, $\bar{c}^i$ is the specific heat capacity, τ is the time, τ_0, τ_1, τ_2 are the relaxation times, Å is a unified parameter which introduced to consolidate all theories into a unified system of equations, $\mathfrak{X}$ is the heat source and $\bar{t}_a$ are the tractions defined by $\bar{t}_a = \sigma_{ab} n_b$, $\bar{d}$ and $\bar{h}$ are the thickness of the substrate and film respectively and $\delta_{\alpha j}$ $(\alpha, j = 1, 2)$ is the Kronecker delta.

A superposed dot denotes differentiation with respect to the time and a comma followed by a subscript denotes partial differentiation with respect to the corresponding coordinates.

For functionally graded materials, the parameters $\bar{C}_{abfg}^i$, $\bar{\beta}_{ab}^i$, $\bar{\mu}^i$, $\bar{\rho}^i$, $\bar{k}_{ab}^i$ and $\bar{k}_{ab}^{i*}$ are space dependent. In this paper, the material is functionally graded along the $0x$ direction. Thus, we replace these quantities by $C_{abfg}^i f(x)$, $\beta_{ab}^i f(x)$, $\mu^i f(x)$, $\rho^i f(x)$, $k_{ab}^i f(x)$ and $k_{ab}^{i*} f(x)$ where C_{abfg}^i, β_{ab}^i, μ^i, ρ^i, k_{ab}^i and k_{ab}^{i*} are assumed to be constants; $i = 1, 2$ represents the parameters in film and substrate, respectively, and $f(x)$ is a given nondimensional function of space variable x. We take $f(x) = (x+1)^m$ where m is a dimensionless constant.

Then the equations (1)-(4) become

$$\sigma_{ab,b} + \tau_{ab,b} - \rho^i (x+1)^m \omega^2 x_a = \rho^i (x+1)^m \ddot{u}_a^i \tag{5}$$

$$\sigma_{ab} = (x+1)^m \left[C_{abfg}^i \aleph u_{f,g}^i - \beta_{ab}^i (T^i - T_0 + \tau_1 \dot{T}^i)\right] \tag{6}$$

$$\tau_{ab} = \mu^i (x+1)^m \left(\tilde{h}_a H_b + \tilde{h}_b H_a - \delta_{ba} (\tilde{h}_f H_f)\right) \tag{7}$$

$$\begin{aligned} &\left[\delta_{1j} k_{ab}^i + \delta_{2j} k_{ab}^{i*}\right] T_{,ab}^i + \rho^i (\mathfrak{X} + \tau_0 \dot{\mathfrak{X}}) \\ &= -\delta_{2j} k_{ab}^i \dot{T}_{,ab}^i + \beta_{ab}^i T_0 \left[Å \delta_{1j} \dot{u}_{a,b}^i + (\tau_0 + \delta_{2j}) \ddot{u}_{a,b}^i\right] + \rho^i c^i (x+1)^m \left[\delta_{1j} \dot{T}^i + (\tau_0 + \delta_{1j} \tau_2 + \delta_{2j}) \ddot{T}^i\right] \end{aligned} \tag{8}$$

Equations (5)-(8) can be reduced to the governing equations of different theories of generalized magneto-thermo-viscoelasticity in a rotating anisotropic FG thin film/substrate structure as follows:

(I) LS: $j = 1$, $Å = 1$ and $\tau_1 = \tau_2 = 0$

(II) GL: $j = 1$, $Å = 1$ and $\tau_0 = 0$

(III) GN III: $j = 2$, $Å = 0$ and $\tau_0 = 0$

Notice that there are two special cases of the GN III theory type, may be obtained by setting $k_{ab}^i \to 0$ and $k_{ab}^{i*} \to 0$, respectively. To obtain the GN theory type II, from the equations of the GN III theory, we set $k_{ab}^i \to 0$. When $k_{ab}^{i*} \to 0$ the equations of the GN III theory reduce to the GN theory type I.

2.1 Initial and boundary conditions

The lower surface of the structure is irradiated by the laser power and temperature of the upper surface of the structure is supposed to be thermal insulation, so that the boundary conditions at these two surfaces can be written as

$$k_S \frac{\partial T_S(0,z,\tau)}{\partial x} = \Gamma_0 \nu(T)\omega(z)\psi(\tau) \tag{9}$$

$$T_F\left(\bar{d}+\bar{h},z,\tau\right) = T_0 \tag{10}$$

where Γ_0 is the incident laser power density, $\nu(T)$ is the optical absorptivity of the film, $\omega(z)$ and $\psi(\tau)$ are the spatial and temporal distribution of the laser pulse.

These two functions can be written as

$$\omega(z) = \exp\left(-\frac{z^2}{a_0^2}\right) \tag{11}$$

$$\psi(\tau) = \frac{\tau}{\tau_3}\exp\left(-\frac{\tau}{\tau_3}\right) \tag{12}$$

where a_0 is the radius of the pulsed laser spot, τ_3 is the rise time of the laser pulse.

Thermal insulation is applied at the z direction, so that

$$k\frac{\partial T(x,0,\tau)}{\partial n} = k\frac{\partial T(x,a,\tau)}{\partial n} \tag{13}$$

Continuity conditions for the temperature, heat flux, displacement and traction at the interface, are as follows

$$T^S(x,z,\tau)\Big|_{x=d} = T^F(x,z,\tau)\Big|_{x=d} \tag{14a}$$

$$q^S(x,z,\tau)\Big|_{x=d} = q^F(x,z,\tau)\Big|_{x=d} \tag{14b}$$

$$u_f^S(x,z,\tau)\Big|_{x=d} = u_f^F(x,z,\tau)\Big|_{x=d} \tag{15a}$$

$$\bar{t}_a^S(x,z,\tau)\Big|_{x=d} = \bar{t}_a^F(x,z,\tau)\Big|_{x=d} \tag{15b}$$

The remaining initial and boundary conditions for the current problem are assumed to be written as

$$u_f^i(x,z,0) = \dot{u}_f^i(x,z,0) = 0 \quad \text{for} \quad (x,z) \in R \cup C \tag{16}$$

$$u_f^i(x,z,\tau) = \Psi_f(x,z,\tau) \quad \text{for} \quad (x,z) \in C_3 \tag{17}$$

$$\bar{t}_a^i(x,z,\tau) = \Phi_f(x,z,\tau) \quad \text{for} \quad (x,z) \in C_4, \tau > 0, \qquad C = C_3 \cup C_4, \quad C_3 \cap C_4 = \emptyset \tag{18}$$

$$T^i(x,z,0) = \dot{T}^i(x,z,0) = 0 \quad \text{for} \quad (x,z) \in R \cup C \tag{19}$$

$$q^i(x,z,\tau) = \bar{h}(x,z,\tau) \quad \text{for} \quad (x,z) \in C_2, \tau > 0, \qquad C = C_1 \cup C_2,\ C_1 \cap C_2 = \emptyset \tag{20}$$

For simplicity in the numerical implementation of DRBEM below, we will drop the superscript i

3 NUMERICAL IMPLEMENTATION

Making use of (6) and (7), we can write (5) as follows

$$L_{gb}u_f = \rho\ddot{u}_a - (D_aT + D_{af} + \Lambda D_{a1f} - \rho\omega^2 x_a) = f_{gb} \tag{21}$$

Where $L_{gb} = D_{abf}\frac{\partial}{\partial x_b}, D_{abf} = C_{abfg}\aleph\varepsilon, \varepsilon = \frac{\partial}{\partial x_g}, D_{af} = \mu H_0^2\left(\frac{\partial}{\partial x_a} + \delta_{a1}\Lambda\right)\frac{\partial}{\partial x_f}, \Lambda = \frac{m}{x+1},$
$D_a = -\beta_{ab}\left(\frac{\partial}{\partial x_b} + \delta_{b1}\Lambda + \tau_1\left(\frac{\partial}{\partial x_b} + \Lambda\right)\frac{\partial}{\partial\tau}\right), f_{gb} = \rho\ddot{u}_a - (D_aT + D_{af} + \Lambda D_{a1f} - \rho\omega^2 x_a).$

The field equations can now be written in operator form as follows

$$L_{gb}u_f = f_{gb} \tag{22}$$

$$L_{ab}T = f_{ab} \tag{23}$$

where the operators L_{gb} and f_{gb} are defined in equation (21), and the operators L_{ab} and f_{ab} are defined as follows:

$$L_{ab} = \left[\delta_{1j}k_{ab} + \delta_{2j}k^*_{ab}\right]\frac{\partial}{\partial x_a}\frac{\partial}{\partial x_b} \tag{24}$$

$$f_{ab} = -\delta_{2j}k_{ab}\dot{T}_{,ab} + \rho c(x+1)^m\left[\delta_{1j}\dot{T} + \left(\tau_0 + \delta_{1j}\tau_2 + \delta_{2j}\right)\ddot{T}\right] + T_0\beta_{ab}\left[\mathring{A}\delta_{1j}\dot{u}_{a,b} + \left(\tau_0 + \delta_{2j}\right)\ddot{u}_{a,b}\right] - \rho(\ddot{\mathfrak{X}} + \tau_0\dddot{\mathfrak{X}}) \tag{25}$$

Using the weighted residual method (WRM), the differential equation (22) is transformed into an integral equation

$$\int_R (L_{gb}u_f - f_{gb})u^*_{da}\,dR = 0 \tag{26}$$

Now, we choose the fundamental solution u^*_{df} as weighting function as follows

$$L_{gb}u^*_{df} = -\delta_{ad}\delta(x,\xi) \tag{27}$$

The corresponding traction field can be written as

$$t^*_{da} = C_{abfg}\aleph u^*_{df,g}n_b \tag{28}$$

The thermoelastic traction vector can be written as follows

$$t_a = \frac{\bar{t}_a}{(x+1)^m} = \aleph\left(C_{abfg}u_{f,g} - \beta_{ab}(T - T_0 + \tau_1\dot{T})\right)n_b \tag{29}$$

Applying integration by parts to (26) using the sifting property of the Dirac distribution, with (27), (28) and (29), we can write the following elastic integral representation formula

$$u_d(\xi) = \int_C (u^*_{da}t_a - t^*_{da}u_a + u^*_{da}\beta_{ab}Tn_b)\,dC - \int_R f_{gb}u^*_{da}dR \tag{30}$$

The fundamental solution T^* of the thermal operator L_{ab}, defined by

$$L_{ab}T^* = -\delta(x,\xi) \tag{31}$$

By implementing the WRM and integration by parts, the differential equation (23) is transformed into the thermal reciprocity equation

$$\int_R (L_{ab}TT^* - L_{ab}T^*T)dR = \int_C (q^*T - qT^*)dC \tag{32}$$

Where the heat fluxes are independent of the elastic field and can be expressed as follows:

$$q = -k_{ab}T_{,b}n_a \tag{33}$$

$$q^* = -k_{ab}T^*_{,b}n_a \tag{34}$$

By the use of sifting property, we obtain from (32) the thermal integral representation formula

$$T(\xi) = \int_C (q^*T - qT^*)dC - \int_R f_{ab}T^*dR \tag{35}$$

The integral representation formulae of elastic and thermal fields (30) and (35) can be combined to form a single equation as follows

$$\begin{bmatrix} u_d(\xi) \\ T(\xi) \end{bmatrix} = \int_C \left\{ - \begin{bmatrix} t^*_{da} & -u^*_{da}\beta_{ab}n_b \\ 0 & -q^* \end{bmatrix} \begin{bmatrix} u_a \\ T \end{bmatrix} + \begin{bmatrix} u^*_{da} & 0 \\ 0 & -T^* \end{bmatrix} \begin{bmatrix} t_a \\ q \end{bmatrix} \right\} dC - \int_R \begin{bmatrix} u^*_{da} & 0 \\ 0 & -T^* \end{bmatrix} \begin{bmatrix} f_{gb} \\ -f_{ab} \end{bmatrix} dR \tag{36}$$

It is convenient to use the contracted notation to introduce generalized thermoelastic vectors and tensors, which contain corresponding elastic and thermal variables as follows:

$$U_A = \begin{cases} u_a & a = A = 1,2,3 \\ T & A = 4 \end{cases} \tag{37}$$

$$T_A = \begin{cases} t_a & a = A = 1,2,3 \\ q & A = 4 \end{cases} \tag{38}$$

$$U^*_{DA} = \begin{cases} u^*_{da} & d = D = 1,2,3; a = A = 1,2,3 \\ 0 & d = D = 1,2,3; A = 4 \\ 0 & D = 4; a = A = 1,2,3 \\ -T^* & D = 4; A = 4 \end{cases} \tag{39}$$

$$\tilde{T}^*_{DA} = \begin{cases} t^*_{da} & d = D = 1,2,3; a = A = 1,2,3 \\ -\tilde{u}^*_d & d = D = 1,2,3; A = 4 \\ 0 & D = 4; a = A = 1,2,3 \\ -q^* & D = 4; A = 4 \end{cases} \tag{40}$$

$$\tilde{u}^*_d = u^*_{da}\beta_{af}n_f \tag{41}$$

Using the contracted notation, the thermoelastic representation formula (36) can be written as:

$$U_D(\xi) = \int_C \left(U^*_{DA}T_A - \tilde{T}_{DA}U_A \right) dC - \int_R U^*_{DA}S_A dR \tag{42}$$

The vector S_A can be written in the split form as follows

$$S_A = S^0_A + S^T_A + S^u_A + S^{\dot{T}}_A + S^{\ddot{T}}_A + S^{\dot{u}}_A + S^{\ddot{u}}_A \tag{43}$$

where

$$S^0_A = \begin{cases} \rho\omega^2 x_a & a = A = 1,2,3 \\ \rho(\ddot{x} + \tau_0\dot{\ddot{x}}) & A = 4 \end{cases} \tag{44}$$

$$S^T_A = \omega_{AF}U_F \qquad \text{with} \quad \omega_{AF} = \begin{cases} -D_a & A = 1,2,3; F = 4 \\ 0 & \text{otherwise} \end{cases} \tag{45}$$

$$S^{\dot{T}}_A = \left(\delta_{2j}k_{ab}\frac{\partial}{\partial x_a}\frac{\partial}{\partial x_b} - c\rho(x+1)^m\delta_{1j} \right)\delta_{AF}\dot{U}_F \text{ with } \delta_{AF} = \begin{cases} 1 & a = A = 4; F = 4 \\ 0 & \text{otherwise} \end{cases} \tag{46}$$

$$S_A^{\ddot{T}} = -c\rho(x+1)^m\left(\tau_0 + \delta_{1j}\tau_2 + \delta_{2j}\right)\delta_{AF}\ddot{U}_F \tag{47}$$

$$S_A^u = -(D_{af} + \Lambda D_{a1f})\mho U_F \qquad \text{with} \quad \mho = \begin{cases} 1 & a = A = 1,2,3; f = F = 1,2,3 \\ 0 & \text{otherwise} \end{cases} \tag{48}$$

$$S_A^{\dot{u}} = -T_0 Å\delta_{1j}\beta_{fg}\varepsilon\dot{U}_F \tag{49}$$

$$S_A^{\ddot{u}} = ⅁\ddot{U}_F \qquad \text{with} \quad ⅁ = \begin{cases} \rho & A = 1,2,3;\ F = 1,2,3, \\ -T_0\beta_{ab}\left(\tau_0 + \delta_{2j}\right)\varepsilon & A = 4; f = F = 4 \end{cases} \tag{50}$$

The thermoelastic representation formula (36) can also be written in matrix form as follows:

$$\begin{aligned}[S_A] = &\begin{bmatrix} \rho\omega^2 x_a \\ \rho(ẍ + \tau_0\dot{ẍ}) \end{bmatrix} + \begin{bmatrix} -D_a T \\ 0 \end{bmatrix} + \begin{bmatrix} -(D_{af} + \Lambda D_{a1f})u_f \\ 0 \end{bmatrix} + \left(\delta_{2j}k_{ab}\frac{\partial}{\partial x_a}\frac{\partial}{\partial x_b} - \rho c(x+1)^m\delta_{1j}\right)\begin{bmatrix} 0 \\ \dot{T} \end{bmatrix} \\ &-\rho c(x+1)^m\left(\tau_0 + \delta_{1j}\tau_2 + \delta_{2j}\right)\begin{bmatrix} 0 \\ \ddot{T} \end{bmatrix} - T_0 Å\delta_{1j}\begin{bmatrix} 0 \\ \beta_{fg}\dot{u}_{f,g} \end{bmatrix} + \begin{bmatrix} \rho\ddot{u}_a \\ -T_0\beta_{fg}\left(\tau_0 + \delta_{2j}\right)\ddot{u}_{f,g} \end{bmatrix}\end{aligned} \tag{51}$$

Our task now is to implement the DRBEM. To transform the domain integral in (42) to the boundary, we approximate the source vector S_A in the domain as usual by a series of given tensor funtions f_{AN}^q and unknown coefficients α_N^q

$$S_A \approx \sum_{q=1}^{N} f_{AN}^q \alpha_N^q \tag{52}$$

Thus, the thermoelastic representation formula (42) can be written in the following form

$$U_D(\xi) = \int_C \left(U_{DA}^* T_A - \tilde{T}_{DA}^* U_A\right)dC - \sum_{q=1}^{N}\int_R U_{DA}^* f_{AN}^q dR\,\alpha_N^q \tag{53}$$

By applying the WRM to the following inhomogeneous elastic and thermal equations:

$$L_{gb}u_{fe}^q = f_{ae}^q \tag{54}$$

$$L_{ab}T^q = f_{pj}^q \tag{55}$$

where the weighting functions are chosen to be the elastic and thermal fundamental solutions u_{da}^* and T^*. Then the elastic and thermal representation formulae are similar to those of Fahmy (2012a) within the context of the uncoupled theory and are given as follows

$$u_{dn}^{q}(\xi) = \int_{C} \left(u_{da}^{*} t_{an}^{q} - t_{da}^{*} u_{an}^{q}\right) dC - \int_{R} u_{da}^{*} f_{an}^{q} dR \tag{56}$$

$$T^{q}(\xi) = \int_{C} \left(q^{*} T^{q} - q^{q} T^{*}\right) dC - \int_{R} f^{q} T^{*} dR \tag{57}$$

The dual representation formulae of elastic and thermal fields can be combined to form a single equation as follows

$$U_{DN}^{q}(\xi) = \int_{C} \left(U_{DA}^{*} T_{AN}^{q} - T_{DA}^{*} U_{AN}^{q}\right) dC - \int_{R} U_{DA}^{*} f_{AN}^{q} dR \tag{58}$$

With the substitution of (58) into (53), the dual reciprocity representation formula of coupled thermoelasticity can be expressed as follows

$$U_{D}(\xi) = \int_{C} \left(U_{DA}^{*} T_{A} - \breve{T}_{DA}^{*} U_{A}\right) dC + \sum_{q=1}^{N} \left(U_{DN}^{q}(\xi) + \int_{C} \left(T_{DA}^{*} U_{AN}^{q} - U_{DA}^{*} T_{AN}^{q}\right) dC \right) \alpha_{N}^{q} \tag{59}$$

To calculate interior stresses, (59) is differentiated with respect to ξ_l as follows

$$\frac{\partial U_{D}(\xi)}{\partial \xi_{l}} = -\int_{C} \left(U_{DA,l}^{*} T_{A} - \breve{T}_{DA,l}^{*} U_{A}\right) dC + \sum_{q=1}^{N} \left(\frac{\partial U_{DN}^{q}(\xi)}{\partial \xi_{l}} - \int_{C} \left(T_{DA,l}^{*} U_{AN}^{q} - U_{DA,l}^{*} T_{AN}^{q}\right) dC \right) \alpha_{N}^{q} \tag{60}$$

According to the steps described in Fahmy (2012b), the dual reciprocity boundary integral equation (59) can be written in the following system of equations

$$\check{\zeta}\check{u} - \eta\check{t} = \left(\zeta\breve{U} - \eta\breve{\varphi}\right)\alpha \tag{61}$$

The technique was proposed by Partridge et al. (1992) can be extended to treat the convective terms, then the generalized displacements U_F and velocities $\dot{U}_F$ are approximated by a series of tensor functions f_{FD}^{q} and unknown coefficients γ_{D}^{q} and $\tilde{\gamma}_{D}^{q}$

$$U_{F} \approx \sum_{q=1}^{N} f_{FD}^{q}(x) \gamma_{D}^{q} \tag{62}$$

$$\dot{U}_{F} \approx \sum_{q=1}^{N} f_{FD}^{q}(x) \tilde{\gamma}_{D}^{q} \tag{63}$$

The gradients of the generalized displacement and velocity can be approximated as follows

$$U_{F,g} \approx \sum_{q=1}^{N} f_{FD,g}^{q}(x)\gamma_K^q \tag{64}$$

$$\dot{U}_{F,g} \approx \sum_{q=1}^{N} f_{FD,g}^{q}(x)\tilde{\gamma}_D^q \tag{65}$$

These approximations are substituted into equations (45) and (49) to approximate the corresponding source terms as follows

$$S_A^T = \sum_{q=1}^{N} S_{AD}^{T,q}\gamma_D^q \tag{66}$$

$$S_A^{\dot{u}} = -T_0 Å\delta_{1j}\beta_{fg}\varepsilon \sum_{q=1}^{N} S_{AD}^{\dot{u},q}\tilde{\gamma}_D^q \tag{67}$$

where

$$S_{AD}^{T,q} = S_{AF} f_{FD,g}^{q} \tag{68}$$

$$S_{AD}^{\dot{u},q} = S_{FA} f_{FD,g}^{q} \tag{69}$$

The same point collocation procedure described in Gaul et al. (2003) can be applied to (52), (62) and (63). This leads to the following system of equations

$$\check{S} = J\alpha, \qquad U = J'\gamma, \qquad \dot{U} = J'\tilde{\gamma} \tag{70}$$

Similarly, the application of the point collocation procedure to the source terms equations (46), (47), (48), (50), (66) and (67) leads to the following system of equations

$$\check{S}^{\dot{T}} = \left(\delta_{2j}k_{ab}\frac{\partial}{\partial x_a}\frac{\partial}{\partial x_b} - \rho c(x+1)^m\delta_{1j}\right)\delta_{AF}\dot{U} \tag{71}$$

$$\check{S}^{\ddot{T}} = -c\rho(x+1)^m\left(\tau_0 + \delta_{1j}\tau_2 + \delta_{2j}\right)\delta_{AF}\ddot{U} \tag{72}$$

$$\check{S}^{u} = -(D_{af} + \Lambda D_{a1f})\mho U_F \qquad \text{with} \quad \mho = \begin{cases} 1 & a = A = 1,2,3; f = F = 1,2,3 \\ 0 & \text{otherwise} \end{cases} \tag{73}$$

$$\check{S}^{\ddot{u}} = \tilde{A}\ddot{U} \tag{74}$$

$$\check{S}^{T} = \mathcal{B}^{T}\gamma \tag{75}$$

$$\check{S}^{\dot{u}} = -T_0 Å \delta_{1j}\beta_{fg}\varepsilon\mathcal{B}^{\dot{u}}\tilde{\gamma} \tag{76}$$

Solving the system (70) for α, γ and $\tilde{\gamma}$ yields

$$\alpha = J^{-1}\check{S} \qquad \gamma = J'^{-1}U \qquad \tilde{\gamma} = J'^{-1}\dot{U} \tag{77}$$

Now, the coefficients α can be expressed in terms of nodal values of the unknown displacements U, velocities $\dot{U}$ and accelerations $\ddot{U}$ as follows:

$$\begin{aligned}\alpha = J^{-1}\Big(\check{S}^{0} + \mathcal{B}^{T}J'^{-1}U + \Big[\Big(\delta_{2j}k_{ab}\frac{\partial}{\partial x_a}\frac{\partial}{\partial x_b} - \rho c(x+1)^{m}\delta_{1j}\Big)\delta_{AF} - T_0 Å\delta_{1j}\beta_{fg}\varepsilon\mathcal{B}^{\dot{u}}J'^{-1}\Big]\dot{U} \\ + \big[\tilde{A} - c\rho(x+1)^{m}(\tau_0 + \delta_{1j}\tau_2 + \delta_{2j})\delta_{AF}\big]\ddot{U}\Big)\end{aligned} \tag{78}$$

where $\tilde{A}$ and $\mathcal{B}^{T}$ are assembled using the submatrices $[Ƌ]$ and ω_{AF} respectively.

An implicit-implicit staggered algorithm was proposed and implemented for use with the DRBEM for solving the generalized magneto-thermoviscoelastic equations which may now be written in a more convenient form after substitution of Eq. (78) into Eq. (61) as follows:

$$\tilde{M}\,\ddot{U}^{i} + \overset{\sim}{\Gamma}\,\dot{U}^{i} + \tilde{K}\,U^{i} = \overset{\sim}{\mathbb{Q}}^{i} \tag{79}$$

$$\tilde{X}\,\ddot{T}^{i} + \tilde{A}\,\dot{T}^{i} + \tilde{B}\,T^{i} = \overset{\sim}{\mathbb{Z}}\,\ddot{U}^{i} + \overset{\sim}{\mathbb{R}}\,\dot{U}^{i} + \tilde{F} \tag{80}$$

where

$$\begin{aligned}&V = \big(\eta\breve{\wp} - \zeta\breve{U}\big)J^{-1}, \quad \overset{\sim}{\Gamma} = V\Big[\Big(k^{i}_{ab}\frac{\partial}{\partial x_a}\frac{\partial}{\partial x_b} - c^{i}\rho^{i}\delta_{1j}\Big)\delta_{AF} - T_0 Å\delta_{1j}\beta^{i}_{ab}\varepsilon\mathcal{B}^{\dot{u}}J'^{-1}\Big],\\ &\tilde{K} = \tilde{\zeta} + V\mathcal{B}^{T}J'^{-1}, \quad \overset{\sim}{\mathbb{Q}} = \eta T + V\check{S}^{0}, \quad \tilde{X} = -\rho^{i}c^{i}(x+1)^{m}\big(\tau_0 + \delta_{1j}\tau_2 + \delta_{2j}\big),\\ &\tilde{M} = V\tilde{A}, \quad \tilde{B} = \delta_{1j}k^{i}_{ab} + \delta_{2j}k^{i*}_{ab}, \quad \overset{\sim}{\mathbb{Z}} = \beta^{i}_{ab}T_0\big(\tau_0 + \delta_{2j}\big),\\ &\overset{\sim}{\mathbb{R}} = \beta^{i}_{ab}T_0 Å\delta_{1j}, \quad \tilde{F} = -\rho^{i}(\mathfrak{X} + \tau_0\dot{\mathfrak{X}}), \quad \tilde{A} = \delta_{2j}k^{i}_{ab}\frac{\partial}{\partial x_a}\frac{\partial}{\partial x_b} - \rho^{i}c^{i}(x+1)^{m}\delta_{1j}.\end{aligned}$$

where $V, \tilde{M}, \overset{\sim}{\Gamma}$ and $\tilde{K}$ represent the volume, mass, damping and stiffness matrices, respectively, $\ddot{U}^{i}, \dot{U}^{i}, U^{i}, T^{i}$ and $\overset{\sim}{\mathbb{Q}}$ represent the acceleration, velocity, displacement, temperature and external force vectors, respectively, $\tilde{A}$, $\tilde{B}$ and $\tilde{F}$ are respectively the capacity and conductivity matrices and the nodal source vector, $\tilde{X}$ is a vector of new material constants proposed by Green and Lindsay (1972) and $\overset{\sim}{\mathbb{Z}}$ and $\overset{\sim}{\mathbb{R}}$ are coupling matrices.

In many applications, the coupling terms $\tilde{\tilde{\mathbb{Z}}}\,\ddot{U}^{i}_{n+1}$ and $\tilde{\tilde{\mathbb{R}}}\,\dot{U}^{i}_{n+1}$ that appear in the heat conduction equation and which are induced by the effect of the strain rate are negligible. Therefore, it is easier to predict the temperature than the displacement. Because the solution of the problem is close to the uncoupled solution. Hence the equations (79) and (80) lead to the following coupled system of differential-algebraic equations (DAEs):

$$\tilde{\tilde{M}}\,\ddot{U}^{i}_{n+1} + \tilde{\tilde{\Gamma}}\,\dot{U}^{i}_{n+1} + \tilde{\tilde{K}}\,U^{i}_{n+1} = \tilde{\tilde{\mathbb{Q}}}^{ip}_{n+1} \tag{81}$$

$$\tilde{\tilde{X}}\,\ddot{T}^{i}_{n+1} + \tilde{\tilde{A}}\,\dot{T}^{i}_{n+1} + \tilde{\tilde{B}}\,T^{i}_{n+1} = \tilde{\tilde{\mathbb{Z}}}\,\ddot{U}^{i}_{n+1} + \tilde{\tilde{\mathbb{R}}}\,\dot{U}^{i}_{n+1} + \tilde{\tilde{F}} \tag{82}$$

where $\tilde{\tilde{\mathbb{Q}}}^{ip}_{n+1} = \eta T^{ip}_{n+1} + V\breve{B}^{0}$ and T^{ip}_{n+1} is the predicted temperature.

Integrating Eq. (79) with the use of trapezoidal rule and Eq. (81), we obtain

$$\dot{U}^{i}_{n+1} = \dot{U}^{i}_{n} + \frac{\Delta\tau}{2}\left(\ddot{U}^{i}_{n+1} + \ddot{U}^{i}_{n}\right) = \dot{U}^{i}_{n} + \frac{\Delta\tau}{2}\left[\ddot{U}^{i}_{n} + \tilde{\tilde{M}}^{-1}\left(\tilde{\tilde{\mathbb{Q}}}^{ip}_{n+1} - \tilde{\tilde{\Gamma}}\,\dot{U}^{i}_{n+1} - \tilde{\tilde{K}}\,U^{i}_{n+1}\right)\right] \tag{83}$$

$$U^{i}_{n+1} = U^{i}_{n} + \frac{\Delta\tau}{2}\left(\dot{U}^{i}_{n+1} + \dot{U}^{i}_{n}\right) = U^{i}_{n} + \Delta\tau\dot{U}^{i}_{n} + \frac{\Delta\tau^{2}}{4}\left[\ddot{U}^{i}_{n} + \tilde{\tilde{M}}^{-1}\left(\tilde{\tilde{\mathbb{Q}}}^{ip}_{n+1} - \tilde{\tilde{\Gamma}}\,\dot{U}^{i}_{n+1} - \tilde{\tilde{K}}\,U^{i}_{n+1}\right)\right] \tag{84}$$

From Eq. (83) we have

$$\dot{U}^{i}_{n+1} = \overline{\Upsilon}^{-1}\left[\dot{U}^{i}_{n} + \frac{\Delta\tau}{2}\left[\ddot{U}^{i}_{n} + \tilde{\tilde{M}}^{-1}\left(\tilde{\tilde{\mathbb{Q}}}^{ip}_{n+1} - \tilde{\tilde{K}}\,U^{i}_{n+1}\right)\right]\right] \tag{85}$$

where $\overline{\Upsilon} = \left(I + \frac{\Delta\tau}{2}\tilde{\tilde{M}}^{-1}\tilde{\tilde{\Gamma}}\right)$

Substituting from Eq. (85) into Eq. (84), we derive

$$\begin{aligned} U^{i}_{n+1} &= U^{i}_{n} + \Delta\tau\dot{U}^{i}_{n} \\ &+ \frac{\Delta\tau^{2}}{4}\left[\ddot{U}^{i}_{n} + \tilde{\tilde{M}}^{-1}\left(\tilde{\tilde{\mathbb{Q}}}^{ip}_{n+1} - \tilde{\tilde{\Gamma}}\,\overline{\Upsilon}^{-1}\left[\dot{U}^{i}_{n} + \frac{\Delta\tau}{2}\left[\ddot{U}^{i}_{n} + \tilde{\tilde{M}}^{-1}\left(\tilde{\tilde{\mathbb{Q}}}^{ip}_{n+1} - \tilde{\tilde{K}}\,U^{i}_{n+1}\right)\right]\right] - * \tilde{\tilde{K}}\,U^{i}_{n+1}\right)\right] \end{aligned} \tag{86}$$

Substituting $\dot{U}^{i}_{n+1}$ from Eq. (85) into Eq. (81) we obtain

$$\ddot{U}^{i}_{n+1} = \tilde{\tilde{M}}^{-1}\left[\tilde{\tilde{\mathbb{Q}}}^{ip}_{n+1} - \tilde{\tilde{\Gamma}}\left[\overline{\Upsilon}^{-1}\left[\dot{U}^{i}_{n} + \frac{\Delta\tau}{2}\left[\ddot{U}^{i}_{n} + \tilde{\tilde{M}}^{-1}\left(\tilde{\tilde{\mathbb{Q}}}^{ip}_{n+1} - \tilde{\tilde{K}}\,U^{i}_{n+1}\right)\right]\right]\right] - \tilde{\tilde{K}}\,U^{i}_{n+1}\right] \tag{87}$$

Integrating the heat equation (80) using the trapezoidal rule, and Eq. (82) we get

$$\dot{T}^{i}_{n+1} = \dot{T}^{i}_{n} + \frac{\Delta\tau}{2}\left(\ddot{T}^{i}_{n+1} + \ddot{T}^{i}_{n}\right) = \dot{T}^{i}_{n} + \frac{\Delta\tau}{2}\left(\tilde{\tilde{X}}^{-1}\left[\tilde{\tilde{\mathbb{Z}}}\,\ddot{U}^{i}_{n+1} + \tilde{\tilde{\mathbb{R}}}\,\dot{U}^{i}_{n+1} - \tilde{\tilde{A}}\,\dot{T}^{i}_{n+1} - \tilde{\tilde{B}}\,T^{i}_{n+1} + \tilde{\tilde{F}}\right] + \ddot{T}^{i}_{n}\right) \tag{88}$$

$$\begin{aligned} T^{i}_{n+1} &= T^{i}_{n} + \frac{\Delta\tau}{2}\left(\dot{T}^{i}_{n+1} + \dot{T}^{i}_{n}\right) \\ &= T^{i}_{n} + \Delta\tau \dot{T}^{i}_{n} + \frac{\Delta\tau^{2}}{4}\left(\ddot{T}^{i}_{n} + \overset{\frown}{X}^{-1}\left[\overset{\frown}{\mathbb{Z}}\,\ddot{U}^{i}_{n+1} + \overset{\frown}{\mathbb{R}}\,\dot{U}^{i}_{n+1} - \overset{\frown}{A}\,\dot{T}^{i}_{n+1} - \overset{\frown}{B}\,T^{i}_{n+1} + \overset{\frown}{F}\right]\right) \end{aligned} \tag{89}$$

From Eq. (88) we get

$$\dot{T}^{i}_{n+1} = \Upsilon^{-1}\left[\dot{T}^{i}_{n} + \frac{\Delta\tau}{2}\left(\overset{\frown}{X}^{-1}\left[\overset{\frown}{\mathbb{Z}}\,\ddot{U}^{i}_{n+1} + \overset{\frown}{\mathbb{R}}\,\dot{U}^{i}_{n+1} - \overset{\frown}{B}\,T^{i}_{n+1} + \overset{\frown}{F}\right] + \ddot{T}^{i}_{n}\right)\right] \tag{90}$$

where $\Upsilon = \left(I + \frac{1}{2}\overset{\frown}{A}\Delta\tau\,\overset{\frown}{X}^{-1}\right)$

Substituting from Eq. (90) into Eq. (89), we have

$$\begin{aligned} T^{i}_{n+1} &= T^{i}_{n} + \Delta\tau \dot{T}^{i}_{n} + \frac{\Delta\tau^{2}}{4}\left(\ddot{T}^{i}_{n} + \overset{\frown}{X}^{-1}\left[\overset{\frown}{\mathbb{Z}}\,\ddot{U}^{i}_{n+1} + \overset{\frown}{\mathbb{R}}\,\dot{U}^{i}_{n+1}\right.\right. \\ &\left.\left. - \overset{\frown}{A}\left(\Upsilon^{-1}\left[\dot{T}^{i}_{n} + \frac{\Delta\tau}{2}\left(\overset{\frown}{X}^{-1}\left[\overset{\frown}{\mathbb{Z}}\,\ddot{U}^{i}_{n+1} + \overset{\frown}{\mathbb{R}}\,\dot{U}^{i}_{n+1} - \overset{\frown}{B}\,T^{i}_{n+1} + \overset{\frown}{F}\right] + \ddot{T}^{i}_{n}\right)\right] - \overset{\frown}{B}\,T^{i}_{n+1} + \overset{\frown}{F}\right)\right) \end{aligned} \tag{91}$$

Substituting $\dot{T}^{i}_{n+1}$ from Eq. (90) into Eq. (82) we obtain

$$\begin{aligned} \ddot{T}^{i}_{n+1} &= \overset{\frown}{X}^{-1}\left[\overset{\frown}{\mathbb{Z}}\,\ddot{U}^{i}_{n+1} + \overset{\frown}{\mathbb{R}}\,\dot{U}^{i}_{n+1}\right. \\ &\left. - \overset{\frown}{A}\left(\Upsilon^{-1}\left[\dot{T}^{i}_{n} + \frac{\Delta\tau}{2}\left(\overset{\frown}{X}^{-1}\left[\overset{\frown}{\mathbb{Z}}\,\ddot{U}^{i}_{n+1} + \overset{\frown}{\mathbb{R}}\,\dot{U}^{i}_{n+1} - \overset{\frown}{B}\,T^{i}_{n+1} + \overset{\frown}{F}\right] + \ddot{T}^{i}_{n}\right)\right] - \overset{\frown}{B}\,T^{i}_{n+1} + \overset{\frown}{F}\right)\right] \end{aligned} \tag{92}$$

Now, a displacement predicted staggered procedure for the solution of (86) and (91) is:

(1) Predict the displacement field: $U^{ip}_{n+1} = U^{i}_{n}$

(2) Substituting for $\dot{U}^{i}_{n+1}$ and $\ddot{U}^{i}_{n+1}$ from equations (83) and (81) respectively in Eq. (91) and solve the resulted equation for the temperature field

(3) correct the displacement field using the computed temperature field for the Eq. (86)

(4) compute $\dot{U}^{i}_{n+1}$, $\ddot{U}^{i}_{n+1}$, $\dot{T}^{i}_{n+1}$ and $\ddot{T}^{i}_{n+1}$ from Eqs. (85), (87), (88) and (92) respectively.

Table 1 Effects of temperature and magnetic field on the wave speed.

Temperature (T)	Magnetic permeability (μ)	Wave speed
50	2	361
40	4	355
30	6	349
20	8	343
10	10	337

To obtain the influence of temperature and magnetic field on the wave speed, we must consider the wave equation

$$\frac{\partial^2 u}{\partial t^2} = v_p^2 \left(\frac{\partial^2 u}{\partial x^2} + \frac{\partial^2 u}{\partial z^2} \right), v_p = \frac{\omega}{\tilde{k}} \tag{93}$$

where v_p is the wave speed and $\tilde{k}$ is a wave number.

Table 2 Effect of anisotropy on the temperature and displacement components.

Temperature (T)		Displacement u_1		Displacement u_2	
isotropic	anisotropic	isotropic	anisotropic	isotropic	anisotropic
50	44.3	0.0233	0.0208	0.0134	0.0105
40	35.2	0.0194	0.0152	0.0117	0.0085
30	26.4	0.0175	0.0137	0.0108	0.0069
20	17.6	0.0169	0.0121	0.0096	0.0048
10	7.8	0.0152	0.0109	0.0089	0.0037

Thus, the results of numerical calculations of these effects in thin film/substrate structure are given in table 1. Also to show the effect of anisotropy on the results, calculations were performed for an isotropic thin film/substrate structure of Salamon (1995) and presented in table 2

4 NUMERICAL RESULTS AND DISCUSSION

Following Fahmy (2012c) monoclinic graphite-epoxy material was chosen as an anisotropic substrate material for the purpose of numerical calculations, and the physical data for which is given as follows:

Elasticity tensor

$$C_{pjkl} = \begin{bmatrix} 430.1 & 130.4 & 18.2 & 0 & 0 & 201.3 \\ 130.4 & 116.7 & 21.0 & 0 & 0 & 70.1 \\ 18.2 & 21.0 & 73.6 & 0 & 0 & 2.4 \\ 0 & 0 & 0 & 19.8 & -8.0 & 0 \\ 0 & 0 & 0 & -8.0 & 29.1 & 0 \\ 201.3 & 70.1 & 2.4 & 0 & 0 & 147.3 \end{bmatrix} \text{GPa}$$

Mechanical temperature coefficient

$$\beta_{pj} = \begin{bmatrix} 1.01 & 2.00 & 0 \\ 2.00 & 1.48 & 0 \\ 0 & 0 & 7.52 \end{bmatrix} \cdot 10^6 \ \text{N/Km}^2$$

Tensor of thermal conductivity is

$$k_{pj} = \begin{bmatrix} 5.2 & 0 & 0 \\ 0 & 7.6 & 0 \\ 0 & 0 & 38.3 \end{bmatrix} \text{W/km}$$

Mass density $\rho = 7820\ \text{kg/m}^3$ and heat capacity $c = 461\ \text{J/(kg K)}$

According to Rasolofosaon and Zinszner (2002) monoclinic North Sea sandstone reservoir rock was chosen as an anisotropic thin film material and physical data are as follows:

Elasticity tensor

$$C_{pjkl} = \begin{bmatrix} 17.77 & 3.78 & 3.76 & 0.24 & -0.28 & 0.03 \\ 3.78 & 19.45 & 4.13 & 0 & 0 & 1.13 \\ 3.76 & 4.13 & 21.79 & 0 & 0 & 0.38 \\ 0 & 0 & 0 & 8.30 & 0.66 & 0 \\ 0 & 0 & 0 & 0.66 & 7.62 & 0 \\ 0.03 & 1.13 & 0.38 & 0 & 0 & 7.77 \end{bmatrix} \text{GPa}$$

Mechanical temperature coefficient

$$\beta_{pj} = \begin{bmatrix} 0.001 & 0.02 & 0 \\ 0.02 & 0.006 & 0 \\ 0 & 0 & 0.05 \end{bmatrix} \cdot 10^6 \ \text{N/Km}^2$$

Tensor of thermal conductivity is

$$k_{pj} = \begin{bmatrix} 1 & 0.1 & 0.2 \\ 0.1 & 1.1 & 0.15 \\ 0.2 & 0.15 & 0.9 \end{bmatrix} \text{W/km}$$

Mass density $\rho = 2216\,\text{kg/m}^3$ and heat capacity $c = 0.1$ J/(kg K), $H_0 = 1000000$ Oersted, $\mu = 0.5$ Gauss/Oersted, $\aleph = 2$, $h = 2$, $\Delta\tau = 0.0001$. The numerical values of the temperature and displacement are obtained by discretizing the boundary into 120 elements ($N_b = 120$) and choosing 60 well spaced out collocation points ($N_i = 60$) in the interior of the solution domain, refer to the recent work of Fahmy (2012d, 2013, 2013a, 2013b).

The initial and boundary conditions considered in the calculations are

$$\text{at } \tau = 0 \qquad u_1 = u_2 = \dot{u}_1 = \dot{u}_2 = 0,\ T = 0 \tag{93}$$

$$\text{at } x = 0 \qquad \frac{\partial u_1}{\partial x} = \frac{\partial u_2}{\partial x} = 0,\ \frac{\partial T}{\partial x} = 0 \tag{94}$$

$$\text{at } x = h + d \qquad \frac{\partial u_1}{\partial x} = \frac{\partial u_2}{\partial x} = 0,\ \frac{\partial T}{\partial x} = 0 \tag{95}$$

$$\text{at } z = 0 \qquad \frac{\partial u_1}{\partial z} = \frac{\partial u_2}{\partial z} = 0,\ \frac{\partial T}{\partial z} = 0 \tag{96}$$

$$\text{at } z = b \qquad \frac{\partial u_1}{\partial z} = \frac{\partial u_2}{\partial z} = 0,\ \frac{\partial T}{\partial z} = 0 \tag{97}$$

where h and d are the thickness of the film and substrate respectively.

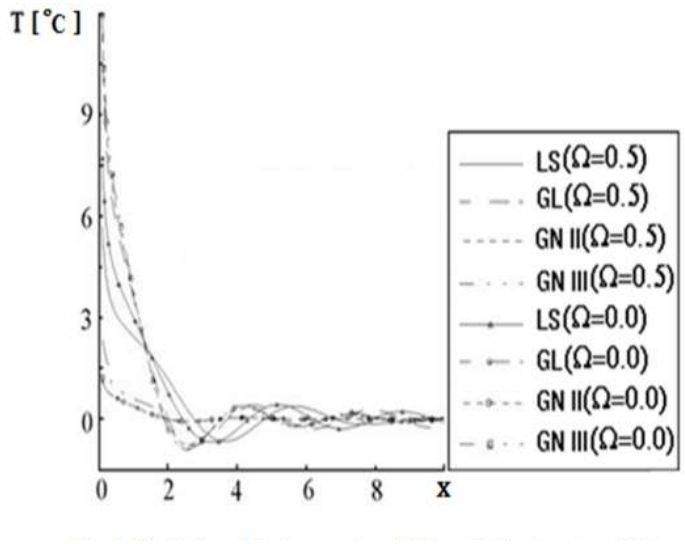

Figure 2 Variation of the temperature T through the structure thickness

Fig. 2 shows that the temperature values near the bottom surface of the substrate for LS and GL theories through the structure thickness in the absence $(\Omega = 0.0)$ of rotation are greater than those in the presence $(\Omega = 0.5)$ of rotation while GN II and GN III theories show the opposite behavior near the bottom surface of the substrate. With a further increase in x, oscillatory patterns for both theories of generalized magneto-thermo-viscoelasticity (LS and GL) take place.

Figs. 3-7 show the influence of the rotation on the displacements (u_1, u_2) and thermal stresses $(\sigma_{11}, \sigma_{12}, \sigma_{22})$ through the structure thickness at $\tau = 0.02, z = 1$. A comparison of the results is presented graphically for generalized theories of magneto-thermo-viscoelasticity in the presence $(\Omega = 0.5)$ and absence $(\Omega = 0.0)$ of rotation.

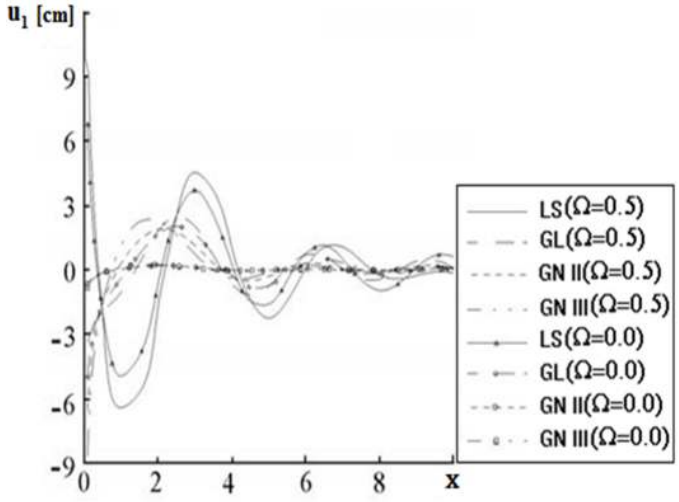

Figure 3 Variation of the temperature u_1 through the structure thickness

Fig. 3 shows that the values of the displacement u_1 near the bottom surface of the structure for the GL and GN III theories through the structure thickness in the absence of rotation are greater than those in the presence of rotation. Also, the effect of rotation may be negligible for the LS theory near the bottom surface of the structure.

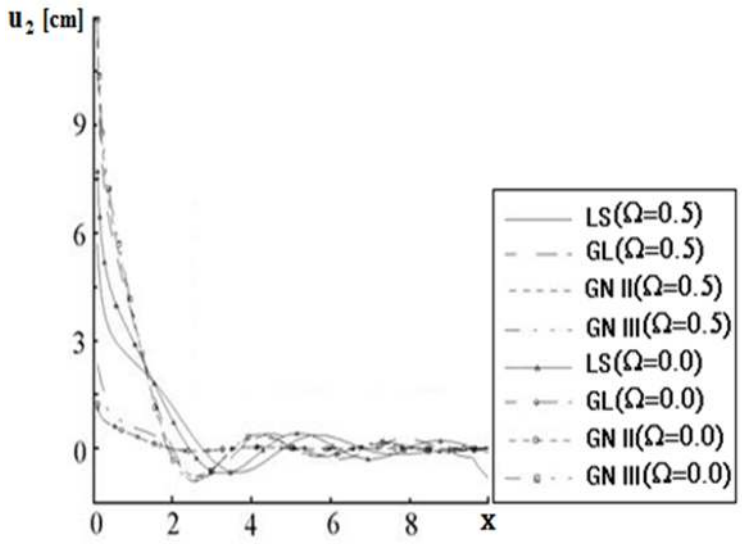

Figure 4 Variation of the temperature u_2 through the structure thickness

Fig. 4 shows that the values of the displacement u_2 near the bottom surface of the structure through-thickness for the LS theory in the absence of rotation are greater than those in the presence of rotation. But for GL theory the values of the displacement u_2 in the presence of rotation are greater than those in the absence of rotation. Also, the effect of rotation in the LS and GL theories is more pronounced than in GN II and GN III. With a further increase in x, oscillatory patterns for all theories of magneto-thermo-viscoelasticity (LS, GL, GN II and GN III) in the absence and presence of rotation take place. These oscillations in the thin film are less clear than in the substrate.
Fig. 5 shows that the values of thermal stress σ_{11} near the bottom surface of the structure for the LS and GL theories in the absence of rotation are greater than those in the presence of rotation. The magnitude of the LS theory in the absence of rotation is higher than those in other theories in the absence and presence of rotation. With a further increase in x, oscillatory patterns for all theories of magneto-thermo-viscoelasticity (LS, GL, GN II and GN III) in the absence and presence of rotation take place. These oscillations are more clear in the absence of rotation than in the presence of rotation.

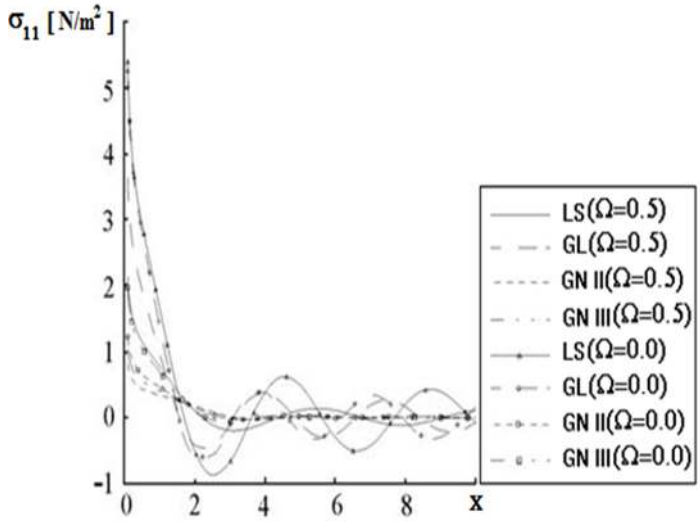

Figure 5 Variation of the thermal stress σ_{11} through the structure thickness

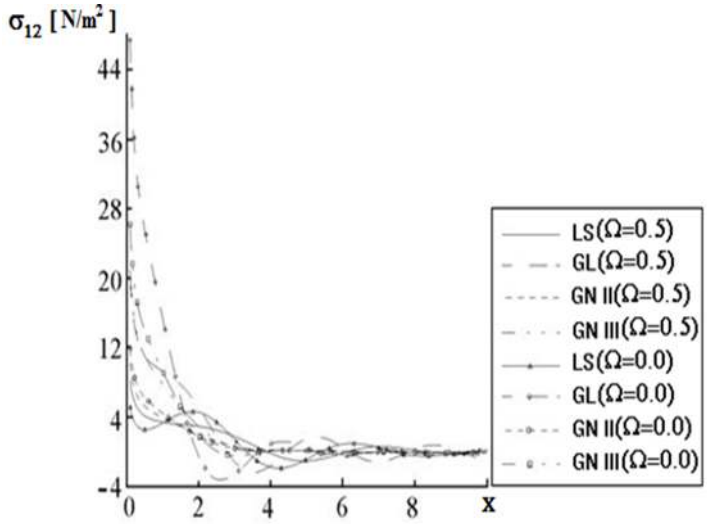

Figure 6 Variation of the thermal stress σ_{12} through the structure thickness

Fig. 6 shows that the values of thermal stress σ_{12} near the bottom surface of the structure for the GL, GN II and GN III theories in the absence of rotation are greater than those in the presence of rotation. But for LS theory in the presence of rotation are greater than those in the absence of rotation. The magnitude of the GL theory in the absence of rotation is higher than those in other theories in the absence and presence of rotation. With a further increase in x, oscillatory patterns for all theories of magneto-thermo-viscoelasticity (LS, GL, GN II and GN III) in the absence and presence of rotation take place. These oscillations are more clear in the substrate for all theories than in the thin film.

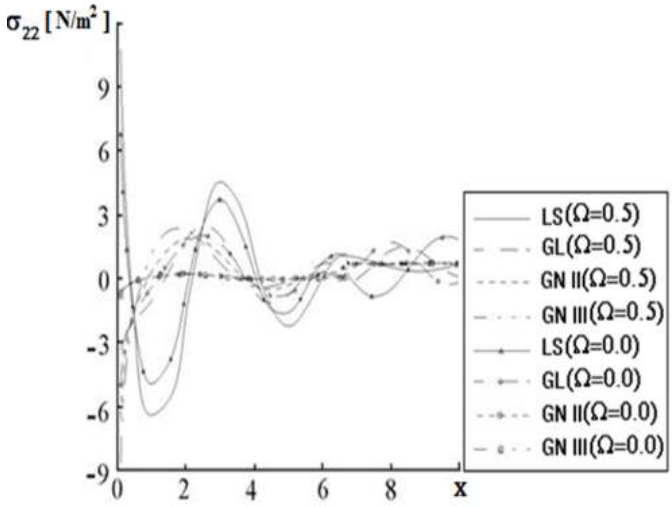

Figure 7 Variation of the thermal stress σ_{22} through the structure thickness

Fig. 7 shows that the values of thermal stress σ_{22} near the bottom surface of the structure for the GL and GN III theories through the structure thickness in the absence of rotation are greater than those in the presence of rotation. Also, the effect of rotation on the thermal stress σ_{22} may be negligible for the LS theory near the bottom surface of the structure. The magnitude of the LS theory in the presence of rotation is higher than those in other theories in the absence and presence of rotation. With a further increase in x, oscillatory patterns for all theories of magneto-thermo-viscoelasticity (LS, GL, GN II and GN III) in the absence and presence of rotation take place. These oscillations are more clear in the substrate for all theories than in the thin film. It is seen that all the figures show that the rotation has a significant effect on the results at small x. Further, beginning from some value of x, the dependences are characterized by oscillations with decreasing magnitudes.

The present work should be applicable to any generalized magneto-thermo-viscoelastic deformation problem. The proposed technique in the present study was discussed in Fahmy [50] who solved the special case from this study in the context of the uncoupled problem. To achieve better efficiency than the technique described in Fahmy (2012d), we use the implicit-implicit algebraic augmentation procedure into a DRBEM code, which is proposed in the current study.

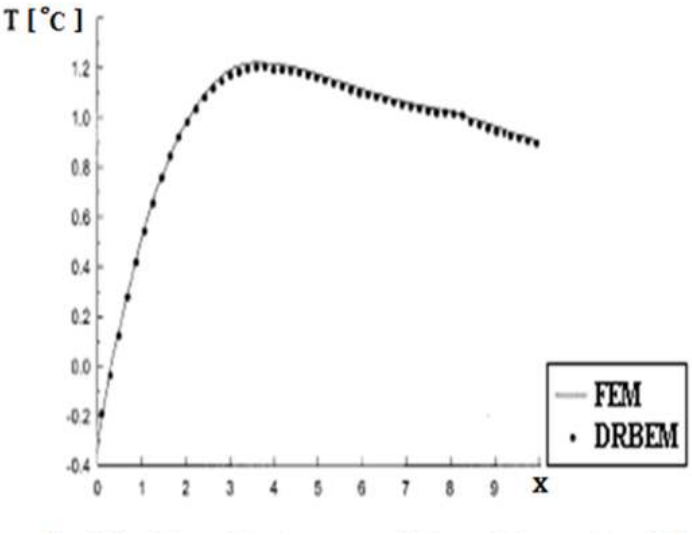

Figure 8 Variation of the temperature T through the structure thickness

The example considered by Xu et al. (2003) may be considered as a special case of the current general problem. In the considered special case, the results of the temperature T are plotted through the structure thickness in Fig. 8 to show the validity of the proposed method. It can be seen from this figure that the DRBEM results of the current study are in excellent agreement with the results obtained by the finite element method (FEM) of Xu et al. (2003).

References

Abd-Alla, A.M., El-Naggar, A.M. and Fahmy, M.A. (2003). Magneto-thermoelastic problem in non-homogeneous isotropic cylinder. Heat and Mass transfer 39: 625-629.

Abd-Alla, A.M., Fahmy, M.A. and El-Shahat, T.M. (2007). Magneto-thermo-elastic stresses in inhomogeneous anisotropic solid in the presence of body force. Far East Journal of Applied Mathematics 27: 499-516.

Abd-Alla, A.M., Fahmy, M.A. and El-Shahat, T.M. (2008). Magneto-thermo-elastic problem of a rotating non-homogeneous anisotropic solid cylinder. Archive of Applied Mechanics 78: 135-148.

Baksi, A., Roy, B.K. and Bera, R.K. (2006). Eigenvalue approach to study the effect of rotation and relaxation time in generalized magneto-thermo-viscoelastic medium in one dimension. Mathematical and Computer Modellin 44: 1069-1079.

Biot, M. (1956). Thermoelasticity and irreversible thermo-dynamics. Journal of Applied Physics 27: 240-253.

Brebbia, C.A., Telles, J.C.F. and Wrobel, L. (1984). Boundary element techniques in Engineering, Springer-Verlag, New York.

Chang, R.C. (2011). Thermoelastic solutions for anisotropic cracked thin films. Thin Solid Films 519: 3225–3235.

Chen, C.H., Chen, C.S., Pan, E., Tseng, H.C. and Yu, P.S. (2009). Boundary element analysis of mixed-mode stress intensity factors in an anisotropic cuboid with an inclined surface crack. Engineering Computations 26: 1056-1073.

Chen, S.C. and Chung, Y.C. (1995). Simulation of the cyclic injection mold-cooling process using dual reciprocity boundary element method. ASME Journal of Heat Transfer 117: 550-553.

Cherepanov, G.P. and Martinez, L. (1997). A computerized model for thermal stresses in thin films. Computers & Structures 63: 1095-1100.

Damanpack, A.R., Bodaghi, M., Ghassemi, H. and Sayehbani, M. (2013). Boundary element method applied to the bending analysis of thin functionally graded plates. Latin American Journal of Solids and Structures 10: 549-570.

Dargush, G.F. and Banerjee, P. K. (1991). A new boundary element method for three-dimensional coupled problems of consolidation and thermoelasticity. ASME Journal of Applied Mechanics 58: 28-36.

Duhamel, J. (1837). Some memoire sur les phenomenes thermo-mechanique. Journal de l'Ecole polytechnique 15: 1-15.

El-Naggar, A.M., Abd-Alla, A.M., Fahmy, M.A. and Ahmed, S.M. (2002). Thermal stresses in a rotating non-homogeneous orthotropic hollow cylinder. Heat and Mass Transfer 39: 41-46.

El-Naggar, A.M., Abd-Alla, A.M. and Fahmy, M.A. (2004). The propagation of thermal stresses in an infinite elastic slab. Applied Mathematics and Computation 157: 307-312.

Fahmy, M.A. (2008). Thermoelastic stresses in a rotating non-homogeneous anisotropic body. Numerical Heat Transfer, Part A 53: 1001-1011.

Fahmy, M.A. (2009). Thermal stresses in a spherical shell under three thermoelastic models using FDM. International Journal of Numerical Methods and Applications 2: 123-128.

Fahmy, M.A. (2010). Application of DRBEM to non-steady state heat conduction in non-homogeneous anisotropic media under various boundary elements. Far East Journal of Mathematical Sciences 43: 83-93.

Fahmy, M.A. (2011). A time-stepping DRBEM for magneto-thermo-viscoelastic interactions in a rotating non-homogeneous anisotropic solid. International Journal of Applied Mechanics 3: 1-24.

Fahmy, M.A. (2011a). Influence of inhomogeneity and initial stress on the transient magneto-thermo-visco-elastic stress waves in an anisotropic solid. World Journal of Mechanics 1: 256-265.

Fahmy, M.A. (2012). Numerical modeling of transient magneto-thermo-viscoelastic waves in a rotating nonhomogeneous anisotropic solid under initial stress. International Journal of Modeling, Simulation and Scientific Computing 3: 125002.

Fahmy, M.A. (2012a). A time-stepping DRBEM for the transient magneto-thermo-visco-elastic stresses in a rotating non-homogeneous anisotropic solid. Engineering Analysis with Boundary Elements 36: 335-345.

Fahmy, M.A. (2012b). Transient magneto-thermoviscoelastic plane waves in a non-homogeneous anisotropic thick strip subjected to a moving heat source. Applied Mathematical Modelling 36: 4565-4578.

Fahmy, M.A. (2012c). Transient magneto-thermo-elastic stresses in an anisotropic viscoelastic solid with and without moving heat source. Numerical Heat Transfer, Part A 61: 547-564.

Fahmy, M.A., (2012d). The effect of rotation and inhomogeneity on the transient magneto-thermo-visco-elastic stresses in an anisotropic solid. ASME Journal of Applied Mechanics 79: 051015.

Fahmy, M.A. (2013). A three-dimensional generalized magneto-thermo-viscoelastic problem of a rotating functionally graded anisotropic solids with and without energy dissipation. Numer. Heat Transfer, Part A: Applications 63: 713-733, 2013.

Fahmy, M.A. (2013a). Generalized magneto-thermo-viscoelastic problems of rotating functionally graded anisotropic plates by the dual reciprocity boundary element method. Journal of Thermal Stresses 36: 1-20, 2013.

Fahmy, M.A. (2013b). Implicit-explicit time integration DRBEM for generalized magneto-thermoelasticity problems of rotating anisotropic viscoelastic functionally graded solids. Engineering Analysis With Boundary Elements 37: 107-115, 2013.

Fahmy, M.A. and El-Shahat, T.M. (2008). The effect of initial stress and inhomogeneity on the thermoelastic stresses in a rotating anisotropic solid. Archive of Applied Mechanics 78: 431-442.

Feng, X., Huang, Y. and Rosakis, A.J. (2008). Stresses in a multilayer thin film/substrate system subjected to nonuniform temperature. ASME Journal of Applied Mechanics 75: 021022.

Gaul, L., Kögl, M. and Wagner, M. (2003). Boundary element methods for engineers and scientists, Springer-Verlag, Berlin.

Green, A.E. and Lindsay, K.A. (1972). Thermoelasticity. Journal of Elasticity 2: 1-7.

Green, A.E. and Naghdi P.M. (1992). On undamped heat waves in an elastic solid. Journal of Thermal Stresses 15: 253-264.

Green, A.E. and Naghdi, P.M. (1993). Thermoelasticity without energy dissipation. Journal of Elasticity 31: 189-208.

Hosseini, S.M., Akhlaghi, M. and Shakeri, M. (2007). Dynamic response and radial wave propagation velocity in thick hollow cylinder made of functionally graded materials. Engineering Computations 24: 288 – 303.

Hsueh, H.C., Chiang, D. and Lee, S. (2010). Modeling of relaxation of viscoelastic stresses in multi-layered thin films/substrate systems due to thermal mismatch. Thin Solid Films 518: 7497–7500.

Huang, Y. and Rosakis, A.J. (2007). Extension of stoney's formula to arbitrary temperature distributions in thin film/substrate systems. ASME Journal of Applied Mechanics 74: 1225-1233.

Lord, H.W. and Shulman, Y. (1967). A generalized dynamical theory of thermoelasticity. Journal of the Mechanics and Physics of Solids 15: 299-309.

Lu, X. and Wu, W.L. (2006). A subregion DRBEM formulation for the dynamic analysis of two-dimensional cracks. Mathematical and Computer Modelling 43: 76-88.

Misra, S.C., Samanta, S.C. and Chakrabarti, A.K. (1992). Transient magnetothermoelastic waves in a viscoelastic half-space produced by ramp-type heating of its surface. Computers & Structures 43: 951-957.

Nardini, D. and Brebbia, C.A. (1983). A new approach to free vibration analysis using boundary elements. Applied Mathematical Modelling 7: 157-162.

Neumann, F. (1885), Vorlesungen Uber die theorie der elasticitat, Meyer, Brestau.

Oden, J.T. and Armstrong, W.H. (1971). Analysis of nonlinear, dynamic coupled thermoviscoelasticity problems by the finite element method. Computers & Structures 4: 603-621.

Xing, H.L. and Makinouchi, A. (2002). FE modeling of thermo-elasto-plastic finite deformation and its application in sheet warm forming. Engineering Computations 19: 392-410.

Othman, M.I.A. and Song, Y. (2008). Effect of rotation on plane waves of generalized electro-magneto-thermoviscoelasticity with two relaxation times. Applied Mathematical Modelling 32: 811–825.

Partridge, P.W. and Brebbia, C.A. (1990). Computer implementation of the BEM dual reciprocity method for the solution of general field equations. Communications in Applied Numerical Methods 6: 83-92.

Partridge, P.W., Brebbia, C.A. and Wrobel, L. C. (1992). The dual reciprocity boundary element method. Computational Mechanics Publications, Boston, Southampton.

Partridge, P.W. and Wrobel, L.C. (1990). The dual reciprocity boundary element method for spontaneous ignition. International Journal for Numerical Methods in Engineering 30: 953–963.

Rafieipour, H., Lotfavar, A., Mahmoodi, E. and Masroori, A. (2013). Application of Laplace Iteration method to Study of Nonlinear Vibration of laminated composite plates. Latin American Journal of Solids and Structures 10: 781-795.

Rasolofosaon, P.N.J., Zinszner, B.E. (2002). Comparison between permeability anisotropy and elasticity anisotropy of reservoir rocks. Geophysics 67: 230-240.

Salamon, N.J. (1995). Bifurcation in isotropic thin film /substrate plates. International Journal of Solids and Structures 32: 473-481.

Ting, E.C. and Chen, H.C. (1982). A unified numerical approach for thermal stress waves. Computers & Structures 15: 165-175.

Tsai, C.C. (2009). The method of fundamental solutions with dual reciprocity for three-dimensional thermoelasticity under arbitrary body forces. Engineering Computations 26: 229 – 244.

Wrobel, L.C., Brebbia, C.A. (1987). The dual reciprocity boundary element formulation for nonlinear diffusion problems. Computer Methods in Applied Mechanics and Engineering 65: 147-164.

Wu, S.K. and Chu, H.S. (2004). Inverse determination of surface temperature in thin-film/substrate systems with interface thermal resistance. International Journal of Heat and Mass Transfer 47: 3507-3515.

Xu, P.Q., Shen, Z.H., Lu, J., Ni, X.W., Zhang, S.Y. (2003). Numerical simulation of laser-induced transient temperature field in film-substrate system by finite element method. International Journal of Heat and Mass Transfer 46: 4963-4968.

Zhou, L. Tang, D., Wu, B. and Qian, H. (2006). Dynamic thermoelastic behavior of metal thin film under transient laser heating. Materials Science and Engineering: A 428: 284–289.